

Multimodal Sensor Fusion for Attitude Estimation of Micromechanical Flying Insects: a Geometric Approach

Domenico Campolo, Luca Schenato, Lijuan Pi, Xinyan Deng and Eugenio Guglielmelli

Abstract—In this paper, we study sensor fusion for the attitude estimation of Micro Aerial Vehicles (MAVs), in particular mechanical flying insects.

First, following a geometric approach, a dynamic observer is proposed which estimates attitude based on kinematic data available from different and redundant bio-inspired sensors such as halteres, ocelli, gravitometers, magnetic compass and light polarization compass. In particular, the traditional structure of complementary filters, suitable for multiple sensor fusion, is specialized to the Lie group of rigid body rotations $SO(3)$.

Then, a numerical implementation of the filter is provided for the specific case of inertial/magnetic navigation, i.e. when gravitometers, magnetometer and gyroscopes are available.

Finally, the filter performance is experimentally tested via a 3 degrees-of-freedom robotic flapper and a custom-made set of inertial/magnetic sensors. Experimental results show good agreement, upon proper tuning of the filter, between the actual kinematics of the robotic flapper and the kinematics reconstructed from the inertial/magnetic sensors via the proposed filter.

Index Terms—sensor fusion, ocelli, halteres, gravitometer, polarization sensor, attitude control, $SO(3)$ Lie group

I. INTRODUCTION

Today there are several successful examples of autonomous flying vehicles, from airplanes [19] to helicopters [20]. However, their size hamper their use in surveillance and search-and-rescue missions in urban areas, in indoor environments and in natural disaster scenarios as after earthquakes. Therefore, there is an increasing need for very small size air vehicles with high performance. In particular, the current trend is to study micro aerial vehicles (MAVs) using traditional air-vehicle paradigms such as fixed-winged air-vehicles [16] or rotorcrafts [21]. Differently, inspired by the unmatched maneuverability and hovering capability by real insects, some groups have started using biomimetic principles to develop micromechanical flying insects (MFIs) with flapping wings that will be capable of sustained autonomous flight [14], [26].

The extraordinary performance of flying insects is the result of two peculiar features: the first feature is the enhanced *unsteady-state aerodynamic* forces and moments generated by the flapping wings [30], [35], [11], and the second feature is the *multimodal sensor fusion*, i.e. the ability

to integrate information from a number of different and redundant sensors to reduce the effect of noise and external disturbances [38], [13].

In this paper, we focus explicitly on the latter feature of insect flight, i.e. on sensor fusion of redundant information for attitude control, and we assume that we can control directly the torque applied to the insect body as shown in [11]. Although sensor fusion and filtering have been studied for decades and many results are available for linear spaces [2], it remains a hard problem on the Lie group of rigid body rotations $SO(3)$ where standard tools like Kalman filtering cannot be applied directly. Theory of complementary and Kalman filters has traditionally been used to design attitude observers, especially in presence of redundant measurements. Kalman filters were originally developed for linear systems and then extended to cope with nonlinearities via linearization techniques. On the other hand, complementary filters are capable of fully exploiting the rich nonlinear structure underlying problems such as rigid body rotations, well described by the theory of Lie groups.

As the main contribution of this work, the traditional structure of complementary filters is specialized to the Lie group of rigid body rotations $SO(3)$. In particular, a dynamic observer is proposed which derives an attitude estimate from redundant information typically available from bio-inspired sensors. Following the geometric approach of [22], [4], [25], this is achieved by avoiding the parametrization step. The proposed observer is based on a notion of state error which is *intrinsic*, so its performance does not depend on an arbitrary choice of coordinates, and *coordinate-free*, in the sense that the equations may be written explicitly without specifying coordinates for the configuration space.

A numerical implementation of the filter is provided for the specific case of inertial/magnetic navigation, i.e. when gravitometers, magnetometer and gyroscopes are available.

As an experimental validation, the filter was used to reconstruct the kinematics of a 3 degrees-of-freedom robotic flapper on which a suite a redundant inertial/magnetic sensors was assembled.

Section II briefly reviews necessary notation, definitions and metric properties concerning the Lie group $SO(3)$ of rigid body rotations. Section III reviews flying insect dynamics and the navigation sensory system of real insects. In Section IV, a complementary filter approach is proposed for sensor fusion. In Section V, the experimental validation of the filter performance is presented.

Corresponding author: d.campolo@unicampus.it

D. Campolo and E. Guglielmelli are with the Biomedical Robotics Laboratory of the Campus Bio-Medico University, 00128 Roma - Italy.

L. Schenato is with the Department of Information Engineering of the University of Padova, 35131 Padova - Italy.

L. Pi and X. Deng are with the Department of Mechanical Engineering, University of Delaware, Newark, DE - USA.

II. MATHEMATICAL BACKGROUND

This section briefly describes the notation and several geometric notions that will be used throughout the paper. For additional details, the reader is referred to texts such as [1], [15], [27], [32], [3].

As shown in [1], [27], the natural configuration space for a rigid body is the *Lie group* $SO(3)$, i.e. the configuration of a rigid body can always be represented by a rotation matrix R , i.e. a matrix such that $R^{-1} = R^T$ and $\det R = +1$. Consider now the coordinate frames \mathbb{R}_S^3 and \mathbb{R}_B^3 :

- $\mathbb{R}_S^3 \approx \mathbb{R}^3$: the *space* coordinate frame, or initial configuration frame.
- $\mathbb{R}_B^3 \approx \mathbb{R}^3$: the *body* frame, which is attached to the body (can be thought of as defined by the sensors sensitive axis), initially coincident with the space frame.

An element R of $SO(3)$ can be thought of as a map from the body frame to the space frame, i.e. $R: \mathbb{R}_B^3 \rightarrow \mathbb{R}_S^3$.

A trajectory of the rigid body is curve $R(t): \mathbb{R} \rightarrow SO(3)$. The velocity vector \dot{R} is tangent to the group $SO(3)$ in R but, as shown in [1], [27], rather than considering \dot{R} , two important quantities are worth to be considered:

- $\dot{R}R^T$: representing the rigid body angular velocity relative to the space frame;
- $R^T\dot{R}$: representing the rigid body angular velocity relative to the body frame.

These are both elements of the *Lie algebra* $so(3)$, i.e. the tangent space to the group $SO(3)$ at the identity I .

Elements of the Lie algebra are represented by skew-symmetric matrices. Systems on Lie groups described in terms of body (space) coordinates are called *left-invariant* (*right-invariant*).

Left-invariance: let $R_1(t)$ be a trajectory of a rigid body relative to a space frame $\mathbb{R}_{S_1}^3$. Consider a change of space frame $G: \mathbb{R}_{S_1}^3 \rightarrow \mathbb{R}_{S_2}^3$, now $R_2(t) = GR_1(t)$ represents the *same* trajectory but with respect to the new space frame. It is straightforward to verify that $R_2^T\dot{R}_2 = R_1^T\dot{R}_1$, i.e. the angular velocity relative to the body frame $R^T\dot{R}$ does not depend on the choice of space frame.

Right-invariance: similarly, it can be shown that the angular velocity of a rigid body relative to a space frame $\dot{R}R^T$ does not depend on the choice of coordinate frame attached to the body.

In the case of $SO(3)$, there exists [27] an isomorphism of vector spaces $\hat{\cdot}: so(3) \rightarrow \mathbb{R}^3$, referred to as *hat* operator, that allows writing $so(3) \approx \mathbb{R}^3$. For a given vector $a = [a_1 \ a_2 \ a_3]^T \in \mathbb{R}^3$, we write:

$$\hat{\cdot}: a = \begin{bmatrix} a_1 \\ a_2 \\ a_3 \end{bmatrix} \longrightarrow \begin{bmatrix} 0 & -a_3 & a_2 \\ a_3 & 0 & -a_1 \\ -a_2 & a_1 & 0 \end{bmatrix} = \hat{a} \quad (1)$$

III. THE SENSORY SYSTEM OF FLYING INSECTS

One reason for superior performance exhibited by flying insects, besides the enhanced unsteady state aerodynamic forces from flapping flight, is the highly specialized sensory system. In order to stabilize flight, insects can rely upon a number of different sensors. In the following, we briefly

review a number of sensors available to insects for navigation, which represent a rich source of inspiration for the mechanical flying insect [7], [10].

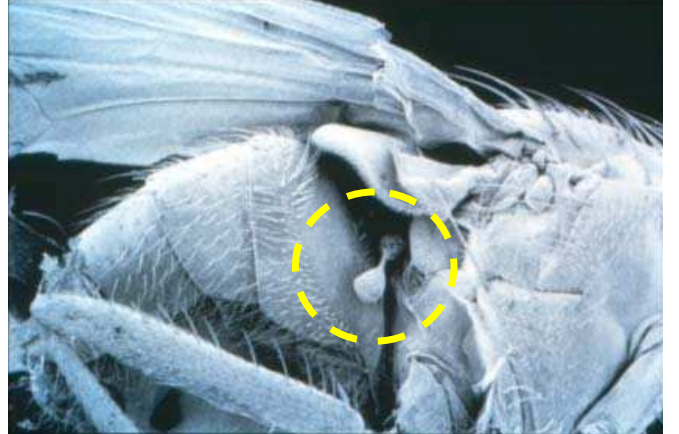


Fig. 1. Photo of a fly haltere. Courtesy of [8].

1) *Halteres:* The halteres are club-shaped small appendages behind each wing that oscillate in anti-phase with respect of the wing, as shown in Fig. 1. The plane of oscillation is slightly tilted toward the tail of the insect to be able to measure Coriolis forces along all three body axes [18]. The halteres function as tiny gyroscopes and through appropriate signal processing [28] they can reconstruct the body angular velocity vector:

$$y_{hl} = \omega \quad (2)$$

Recently, preliminary prototypes of micro-electromechanical halteres have been fabricated and have shown promising results [39].

2) *Mechanoreceptors:* Insects wings and other parts of the body such as the antennae, neck and legs are innervated by campaniform sensilla. These nerves can sense and encode pressure forces when they are stretched or strained [12]. In particular, the sensilla on the legs can be used to measure the gravity sensor, thus acting as a gravimeter. Therefore, we can assume that insect can measure the gravity vector with respect to the body frame, i.e.

$$y_g = R^T g_0 \quad (3)$$

where g_0 are the (known) gravity vector components, measured with respect to the fixed frame.

3) *Ocelli:* The ocelli are three additional light-sensitive organs that look forward, leftward and rightward, respectively, located in the middle of the compound eyes as shown in Fig. 2 and provide signals that are used for stabilization with respect to rapid perturbations in roll and pitch [7]. In fact, these sensor can estimate the position of the sun with respect to insect body by comparing the signals from the left and right ocelli to estimate the roll angle, and by comparing the signal from the forward-looking ocellus with the mean of the signals from the left and the right ocelli to estimate the pitch angle [34].

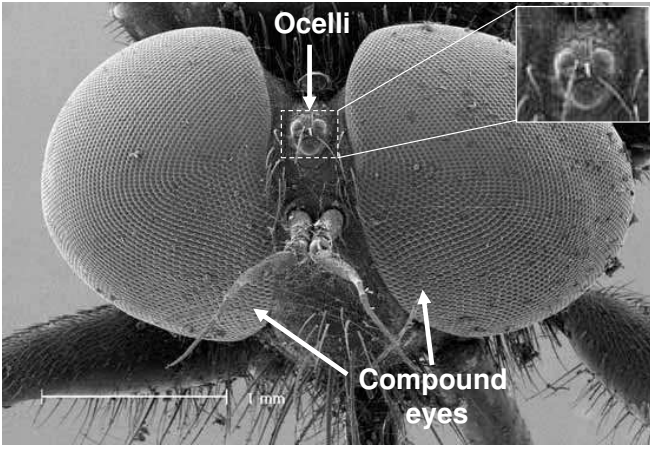


Fig. 2. Photo of fly's head showing compound eyes and the ocelli with its three photoreceptors. Courtesy of [36].

4) *Compound eyes*: The compound eyes of the insects provides different types of signals needed for the optomotor systems. They provide computation of insect angular velocities accomplished by using large-field neurons that are tuned to respond to the specific patterns of optic flow that are generated by yaw, roll and pitch [29]. Compound eyes precisely estimate angular velocities at low frequencies. The compound eyes can also estimate body orientation and position by higher level visual processing like object fixation and landmarks detection for navigation and path planning [13]. Finally, the dorsally directed (upward-looking) regions of the compound eyes of many insects are equipped with specialized photoreceptors that are sensitive to the polarized light patterns that are created by the sun in the sky. More precisely insects can measure their orientation relative to the direction of the light polarization: $p_0 \in \mathbb{R}^3$, as:

$$y_p = R^T p_0 \quad (4)$$

Differently from the ocelli, the light polarization direction is not affected by light intensity. Bio-inspired polarized light compasses have been successfully fabricated and used for robot navigation [23].

5) *Magnetic compass*: Recent studies indicate that some insects also possess a magnetic sense that informs them of their heading direction, and helps them maintain it [37]. Similarly to the light polarization sensor, we can argue that insect can measure the components of the magnetic field with respect to the body as follows:

$$y_m = R^T b_0 \quad (5)$$

where $b_0 \in \mathbb{R}^3$ is the direction of magnetic field relative to the fixed frame. A possible electromechanical implementation of a magnetic compass suitable for small size vehicles is given in [40].

IV. SENSOR FUSION VIA COMPLEMENTARY FILTERS

The sensory system of real insects is clearly redundant, i.e. kinematic quantities such as the angular velocity are de-

rived from more than one sensor. Information from different sensors is then “fused” together.

Complementary filters traditionally arise in applications where redundant measurements of the same signal are available [2] and the problem is combining all available information in order to minimize the instrumentation error.

For sake of simplicity, consider only two sensors, s_1 and s_2 , providing readings of the *same* quantity, e.g. the angular velocity ω , with different noise characteristics, i.e. $s_1 = \omega + n_1$ and $s_2 = \omega + n_2$, where $\|n_1\| < \|n_2\|$ at high frequency while $\|n_2\| < \|n_1\|$ at low frequency.

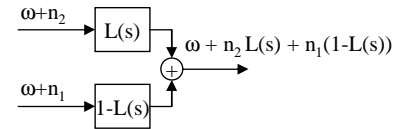


Fig. 3. Sensor fusion via a complementary filter. The low-pass is $L(s)$ while the high-pass is defined as $1 - L(s)$, in this sense the filter is “complementary”.

Complementary filters such as the one in Fig. 3 can be used to fuse information from two or more sensors (e.g. halteres, ocelli and compound eyes) with the characteristic of sensing the *same* variable (e.g. angular velocity) although being subject to noise and disturbances with different spectral content [2].

Remark 1 (non-dynamic estimation): The kinematic variable (ω in Fig. 3) is dynamically *unaffected* by the filter. The estimated variable (i.e. the output of the filter) is related to the input variable via a purely algebraic relation in the time domain and no dynamics are involved in the noiseless case.

Such filters can be safely used in feedback loops to fuse readings of the *same* kinematic variable from different sensors since no extra dynamics is added to the overall system and stability (which involves noiseless conditions) is not affected.

Complementary filters can be generalized to fuse information deriving from sensors when the sensed variables are related by differential equations, i.e. the filter introduces some dynamics between the estimated output and the sensed inputs.

The differential equations relating the sensed variables may be nonlinear, this is typically the case when attitude is concerned. Theory of complementary and Kalman filters has been traditionally been used to design attitude filters. Although the Kalman filters can be extended (EKF) to nonlinear cases, they fail in capturing the nonlinear structure of the configuration space of problems involving, for example, rotations of a rigid body, and most importantly, they can run into instabilities. On the other hand, nonlinear filters [9], in particular complementary filters, can better capture such a nonlinear structure.

A. Dynamic Attitude Estimation

As an example of use of complementary filters when *different* kinematic variables are involved, consider the linear

case of a rotational mechanical system with one degree of freedom (θ). As shown in [2], complementary filters such as the one represented in Fig. 4 are traditionally used to fuse information available from both angular position sensors and tachometers, respectively θ_{sens} and ω_{tacho} . Let θ^* be the estimate of θ . The filter gain k in Fig. 4 determines the transition frequency of the filter after which the data from the tachometer (ω_{tacho}) are weighted more whereas before the transition frequency data from the position sensors (θ_{sens}) are predominant on the dynamic equation (the integrator $1/s$). The optimal value for k is in fact determined by the characteristics of measurement noise, see [2].

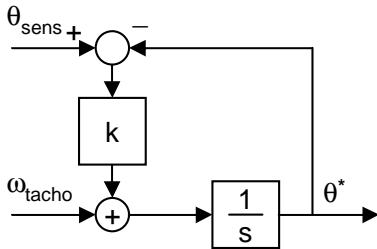


Fig. 4. Linear complementary filter for a rotational mechanical system with one degree of freedom.

Differently from previous example, $SO(3)$ is a *nonlinear* space and that is where the advantages of a geometric approach can be fully appreciated. Besides nonlinear dynamics, the very definition of estimation error requires caution. In the linear case $e = \theta - \theta^*$ is a typical choice while quantities such as $R - R^*$ with $R, R^* \in SO(3)$ are no longer guaranteed to belong to $SO(3)$. Following [5], the estimation error will be defined as $E = R^T R^*$.

Next, a complementary filter on $SO(3)$ for dynamic attitude estimation is presented which fuses information from gyroscopes and from different and possibly redundant navigation sensors, such as the ones described in Section III.

B. Complementary filtering on $SO(3)$

Consider $N \geq 2$ homogenous and time-invariant vector fields $\vec{v}_1, \vec{v}_2, \dots, \vec{v}_N$ (e.g. the gravitational field, the geomagnetic field, the light direction etc...) without the need, for the moment, to specify their components (therefore the symbol $\vec{\cdot}$). Assume that at least two of them (e. g. \vec{v}_1 and \vec{v}_2 , without loss of generality) are independent, this can be expressed in a form that is invariant and coordinate-free:

$$\vec{v}_1 \times \vec{v}_2 \neq 0 \quad (6)$$

Given a rigid body, define a body frame \mathcal{B} on it. Let the rigid body be at rest at some time t_0 and define thus a space frame \mathcal{S}_0 as the one coincident with the body frame \mathcal{B} at time t_0 . Let the constant vectors $v_{i0} = [v_{i0x} \ v_{i0y} \ v_{i0z}]^T$ represent the components of each vector field at time t_0 as measured by a set of sensors on the rigid body. At any time t , let $R(t) : \mathbb{R} \rightarrow SO(3)$ be a twice-differentiable function representing the orientation of the rigid body in 3D space with respect to the space frame \mathcal{S}_0 , let $v_i = [v_{ix} \ v_{iy} \ v_{iz}]^T$ be the (time-variant) components of each field and let ω_{gyr}

be readouts of the gyroscopes, both v_i and ω_{gyr} are referred to the (body) moving frame.

The trajectory $R(t) \in SO(3)$, as defined above, is reflected in the measurements of the gyroscopes and of the vector fields sensors and can be expressed as

$$\begin{cases} \hat{\omega}_{gyr} &= R^T \dot{R} = \hat{\omega} \\ v_i &= R^T v_{0i} \end{cases} \quad (7)$$

Theorem 1: Let $R(t) : \mathbb{R} \rightarrow SO(3)$ represent the orientation of the rigid body. Let $R^*(t)$ denote the estimate of $R(t)$ and let it be defined by the following observer:

$$\begin{cases} \dot{R}^* &= R^* \hat{\omega}^* \\ \omega^* &= \omega_{gyr} + \sum_{i=1}^N k_i (v_i \times v_i^*) \\ v_i^* &= R^{*T} v_{0i} \end{cases} \quad (8)$$

where $k_i > 0$ are the filter gains, ω_{gyr} and v_i represent the sensor readings as in (7).

The observer (8) asymptotically tracks $R(t)$ for almost any initial condition $R^*(0) \neq R(0)$ and in particular:

$$\lim_{t \rightarrow \infty} R^T(t) R^*(t) = I \quad (9)$$

The theorem is stated in a form which is similar to [17], where a possible proof can also be found. Independently from [17], we developed a proof which extends our previous work [6], based on a geometrical approach. In our proof, too lengthy to be presented here, we clearly distinguish the role of gyroscopes from the other sensors, coming to a more general conclusion summarized in the following remark.

Remark 2: Gyroscopes, in fact, are not necessary for stability, at least when tracking a certain (large) subset of trajectories of interest, for which the measurements of 2 vector fields such as the gravitational and the geomagnetic ones are sufficient [6], but knowledge of the angular velocity is beneficial for performance, especially when disturbances are present.

Remark 3: The proposed filter, see next section for an implementation, can be still used for stable tracking when the information from gyroscopes is completely or partially missing (e.g. only mono-axial or bi-axial gyroscopes are available, as for the case of the halteres), of course with a worsening of the performance.

C. Filter Implementation

In this section, the implementation for the specific case of two vector fields $v_1 = g$ and $v_2 = b$, with setup measurements $v_{01} = g_0$ and $v_{02} = b_0$, together with data from gyroscopes (ω_{gyr}), is presented. In particular, Fig. 5 shows the general observer (8) in terms of block diagrams which can be directly implemented in simulation environments such as MATLAB/Simulink from MathWorks Inc.

The diagram in Fig. 5, in particular the integration block $1/s$, is a continuous-time filter. Any digital implementation of the filter would *i*) transform the filter in a discrete-time one with time sequence t_n and *ii*) necessarily introduce numerical errors. The main risk is that, as numerical errors accumulate, quantities such as $R_n^* = R^*(t_n)$ are likely to

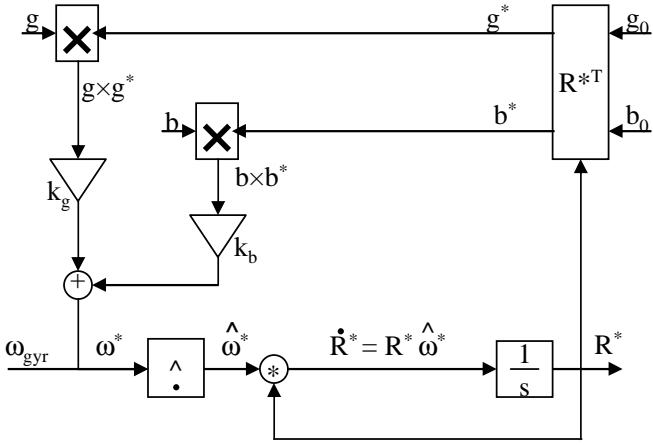


Fig. 5. Complementary filter for dynamic attitude estimation.

drift away from $SO(3)$, i.e. $\det R_n^*$ very different from 1 and/or $R_n^{*T} R_n^*$ very different from the identity matrix I . This can be avoided by considering that data from analog sensors are typically acquired via DACs (Digital to Analog Converters) with a fixed sampling time, let this sampling time be ΔT . In the time interval $t_n \leq t < t_{n+1} = t_n + \Delta T$, data from sensors are assumed constant, i.e. $\omega(t) = \omega_n$, $g(t) = g_n$ and $b(t) = b_n$. This allows computing R_{n+1}^* via the Rodrigues' formula [27] as:

$$\begin{aligned} \omega_n^* &= \omega_n + k_b(g_n \times (R_n^{*T} g_0)) + k_b(b_n \times (R_n^{*T} b_0)) \\ \alpha_n &= \sin \|\Delta T \hat{\omega}_n^*\| / \|\Delta T \hat{\omega}_n^*\| \\ \beta_n &= (1 - \cos \|\Delta T \hat{\omega}_n^*\|) / \|\Delta T \hat{\omega}_n^*\|^2 \\ R_{n+1}^* &= R_n^* (I + \alpha_n \Delta T \hat{\omega}_n^* + \beta_n \Delta T \hat{\omega}_n^{*2}) \end{aligned} \quad (10)$$

which is guaranteed *not* to drift away from $SO(3)$.

Remark 4 (sensor fusion on the Lie algebra): in linear cases as in Fig. 4, all the variables belong to the same space \mathbb{R}^n while, in the nonlinear filter in Fig. 5, variables in different nodes of the block diagram belong to very different spaces, some linear ($so(3)$) and some nonlinear ($SO(3)$). The adopted geometric approach leads to recognize how sensor fusion *naturally* occurs on the linear space of angular velocities, i.e. the Lie algebra $so(3)$.

V. EXPERIMENTAL RESULTS

In this section, the experimental results relative to attitude estimation of the end-effector of a robotic flapper are presented.

A. Experimental Setup

A robotic wrist was designed to generate motion in three independent rotational degrees of freedom. A bevel gear wrist mechanism was developed to transmit the motion of coaxial drive shafts to the plate holder as shown in Fig. 6. The roll and pitch ranges do not have any limits, but the yaw angle was constrained to 45° in our mechanical wrist. Drive shafts were powered by Maxon 16mm DC brush motors with planetary gearheads and magnetic encoders. Gearhead reductions were 19:1 for yaw and pitch, and 84:1 for roll. All three motors have been upgraded to 84:1 gearheads. The

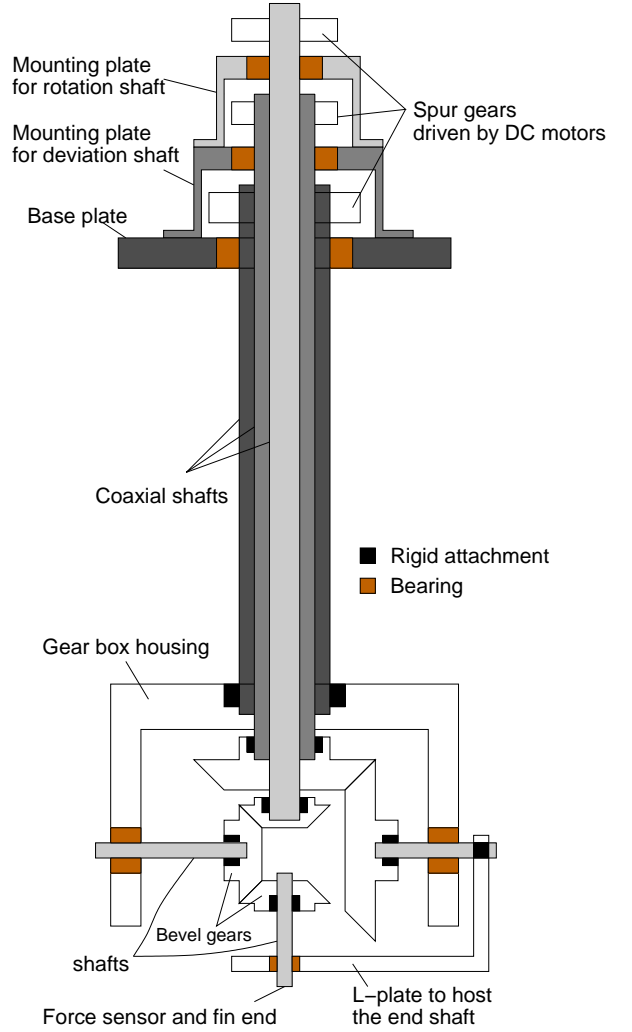


Fig. 6. Design layout of the first generation 3DOF mechanical flapper (not to scale)

mechanism itself saw gear ratios (drive to driven) of 4:1 for roll, 8:1 for yaw, and 1:1 for pitch. The wrist mechanism was reduced in size (roughly 1.5" x 1.5" x 1.25") to accommodate greater motion. A parallel plate mounting structure for the motors makes the setup compact and portable (see Fig. 6). The design allows for quick and easy changing of sensor plate. The motors were driven from MATLAB Simulink models, which used an additional toolbox provided by the control board manufacturer (Quanser consulting) to communicate with the hardware. PID controllers were used to run the motors at a high level of precision: up to a tenth of a degree. Motion commands from the computer were amplified by analog amplifier units (Advanced Motion Control) running in torque mode, which directly controls the input current that the motor receives in order to perform a given motion.

As for the sensors, we used the Honeywell HMC2003 high sensitivity, three-axis magnetic sensor to measure low magnetic field strengths, such the geomagnetic field. The sensitivity is 1V/gauss and the bandwidth is 1 kHz. The micro

accelerometer we used is ADXL330 (from Analog Devices) which is a small, thin, low power 3-axis accelerometer with signal conditioned voltage outputs all on a single monolithic IC. It measures acceleration with range of up to 3g. It can measure the static acceleration of gravity, as well as dynamic acceleration resulting from motion. Bandwidth has a range of 0.5 Hz to 1600 Hz for X and Y axes, and a range of 0.5 Hz to 550 Hz for the Z axis. The sensitivity each axis is 300 mV/g with good linearity. For angular rate sensor, we used IDG-300 (from InvenSense), an integrated 2-axis angular rate sensor (gyroscope). Two chips of IDG-300 was used to make a 3-axis gyroscope system, and the bandwidth is 140Hz.

B. Results

The sensors were assembled and mounted on the plate attached to the robotic wrist. Angular motions in roll, pitch, yaw were performed independently and real time sensor output was obtained from the data acquisition systems and the sensor fusion algorithm results are compared with the actual wrist motion (read from the motor encoder).

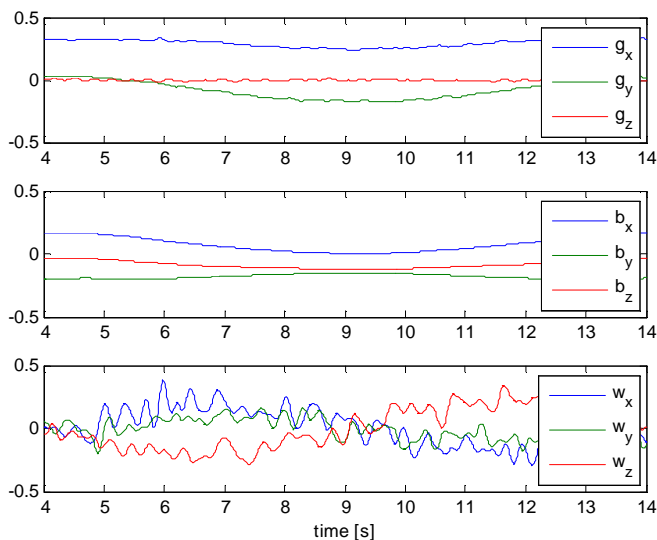


Fig. 7. Normalized calibrated data from sensors.

Coupled motions with multiple degrees of freedom were also performed, calibrated data from sensors derived from a particular motion are shown in Fig. (7). Experimental results are promising in the sense that the actual motion can be reconstructed after proper tuning of the filter (i.e. after choosing appropriate gain values). Fig. (8) shows the estimate of a particular angle (ϕ) during a motion of the robotic flapper which involved all the 3 degrees of freedom.

Note, in Fig. (7), that the actual sensor data from the test have high frequency oscillations which is due to the plate vibration during acceleration, this can be reduced by mounting the sensors on a shorter plate therefore reduce the load induced torque on the gearbox.

VI. CONCLUSION

In this work, we present a geometric, i.e. intrinsic and coordinate-free, approach to attitude estimation of a mi-

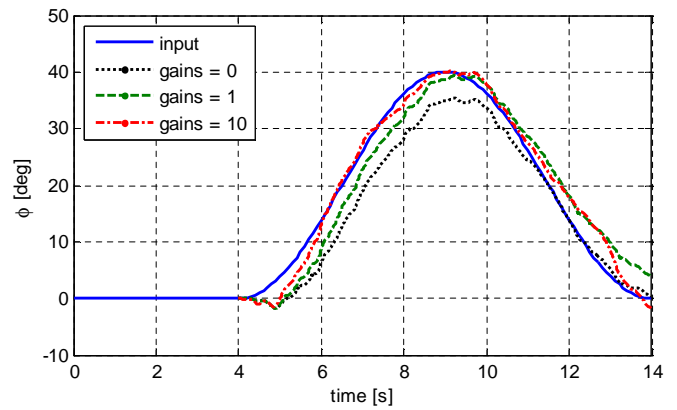


Fig. 8. The angular motion, as desired input (solid line) to the high precision motors servo system, can be reconstructed from calibrated data via the complementary filter algorithm.

cro-mechanical flying insect, derived from multiple and possibly redundant bio-inspired navigation sensors.

Such a multimodal sensor fusion is implemented by a dynamic observer, in particular a complementary filter is proposed which is specialized to the nonlinear structure of the Lie group of rigid body rotations.

The numerical implementation is also provided in the specific case of interest for inertial/magnetic navigation, i.e. when gravimeters, magnetometers and gyroscopes are available.

The proposed filter was experimentally tested. In particular, a 3 degrees of freedom robotic flapper was used to generate a known trajectory. A custom-made suite of inertial/magnetic sensors was assembled on the end-effector of the robotic flapper and the filter was used to estimate the actual (known) motion of the robotic flapper.

As future work, convergence properties of the proposed observer will be analyzed in presence of noisy data and disturbances (e.g. non-inertial accelerations, geomagnetic field distortion etc...). The filter will be also tested in more realistic conditions: miniaturized inertial/magnetic systems will be mounted onboard of small flying vehicles as well as biomimetic swimming robots.

REFERENCES

- [1] V. I. Arnold, "Mathematical Methods of Classical Mechanics", 2nd ed., Springer-Verlag, New York, 1989.
- [2] R. G. Brown and P. Y. C. Hwang, "Introduction to random signals and applied Kalman filtering", New York: J. Wiley, 1992.
- [3] F. Bullo and A. D. Lewis, "Geometric Control of Mechanical Systems", Springer, 2005.
- [4] F. Bullo and R. M. Murray, "Tracking for Fully Actuated Mechanical Systems: a Geometric Framework", Automatica, Vol. 35, No. 1, pp. 17-34 Jan. 1999.
- [5] F. Bullo and R. F. Murray "Proportional derivative (PD) Control on the Euclidean Group", Technical report, California Institute of Technology, Anaheim, CA USA, 1995.
- [6] D. Campolo, F. Keller, E. Guglielmelli, "Inertial/Magnetic Sensors Based Orientation Tracking on the Group of Rigid Body Rotations with Application to Wearable Devices", IEEE/RSJ Int. Conf. on Intelligent Robots and Systems (IROS), Beijing, P.R. China, October 9-14, 2006.

- [7] J. Chahl, "Bioinspired Engineering of Exploration Systems: A Horizon Sensor/Attitude Reference System Based on the Dragonfly Ocelli for Mars Exploration Applications", *Journal of Robotic Systems*, Vol. 20, No. 1, pp. 35-42 2003.
- [8] Commonwealth Scientific and Industrial Research Organisation (CSIRO), URL: <http://www.csiro.au/>.
- [9] F. Daum, "Nonlinear Filters: Beyond the Kalman Filter", *IEEE A&E Systems Magazine*, Vol.20, No. 8, August 2005.
- [10] X. Deng and L. Schenato and W.C. Wu and S.S. Sastry, "Flapping Flight for Biomimetic Robotic Insects. Part I: System modeling", *IEEE Transactions on Robotics*, Vol. 22, No. 4, pp. 789- 803, 2006.
- [11] X. Deng and L. Schenato and S.S. Sastry, "Flapping Flight for Biomimetic robotic Insects. Part II: Flight Control Design", *IEEE Transactions on Robotics*, Vol. 22, No. 4, pp. 789- 803, 2006.
- [12] M.H. Dickinson, "Linear and nonlinear encoding properties of an identified mechanoreceptor on the fly wing measured with mechanical noise stimuli", *The Journal of Experimental Biology*, Vol. 151, pp. 219-244, 1990.
- [13] M. Epstein, S. Waydo, S.B. Fuller, W. Dickson, A. Straw, M.H. Dickinson, and R.M. Murray, "Biologically Inspired Feedback Design for *Drosophila* Flight", to appear in Proc. of IEEE American Control Conference, 2007.
- [14] R.S. Fearing, K.H. Chiang, M.H. Dickinson, D.L. Pick, M. Sitti, J. Yan, "Wing Transmission for a Micromechanical Flying Insect", in Proc. of IEEE Intl. Conf. on Robotics and Automation, pp. 1509-1516, 2000.
- [15] T. Frankel, "The Geometry of Physics: an Introduction", Cambridge University Press, Cambridge, UK, 1997.
- [16] J. Grasmeyer and M.T. Keennon, "Development of the black widow micro air vehicle", in 39th AIAA Aerospace Sciences Meeting and Exhibit, 2001.
- [17] T. Hamel and R. Mahony, "Attitude estimation on $SO(3)$ based on direct inertial measurements", in Proc. of IEEE Intl. Conf. on Robotics and Automation (ICRA), 2006.
- [18] R. Hengstenberg, "Mechanosensory control of compensatory head roll during flight in the blowfly *Calliphora erythrocephala*", *Journal of Comparative Physiology A-Sensory Neural & Behavioral Physiology*, Vol. 163, pp. 151-165, 1988.
- [19] J.P. How, E. King, and Y. Kuwata, "Flight Demonstrations of Cooperative Control for UAV Teams", in AIAA 3rd Unmanned Unlimited Technical Conference, pp. 1509-1516, 2004.
- [20] H.J. Kim and D.H. Shim and S.Sastry, "A Flight Control System for Aerial Robots: Algorithms and Experiments", *Control Engineering Practice*, Vol. 11, No. 12, pp. 1389-1400, 2003.
- [21] I. Kroo and P. Kunz, "Development of the Mesicopter: A Miniature Autonomous Rotorcraft", in American Helicopter Society (AHS) Vertical Lift Aircraft Design Conference, 2000.
- [22] D. E. Koditschek, "The application of total energy as a Lyapunov function for mechanical control systems", in J. E. Marsden, P. S. Krishnaprasad & J. C. Simo (eds), *Dynamics and Control of Multibody Systems*, Vol. 97, AMS, pp. 131-157, 1989.
- [23] D. Lambrinos, H. Kobayashi, R. Pfeifer, M. Maris, T. Labhart, R. Wehner, "Adaptive Behavior An Autonomous Agent Navigating with a Polarized Light Compass", *Adaptive Behavior*, Vol. 6, No. 1, pp. 131-161, 1997.
- [24] D. H. S. Maithripala, J. M. Berg, and W. P. Dayawansa, "Almost-Global Tracking of Simple Mechanical Systems on a General Class of Lie Groups", *IEEE Trans. on Automatic Control*, Vol. 51, No. 1, Jan. 2006.
- [25] D. H. S. Maithripala, J. M. Berg and W. P. Dayawansa, "An Intrinsic Observer for a Class of Simple Mechanical Systems on a Lie Group", *SIAM Journ. Control Optim.*, Vol. 44, No. 5, pp. 1691-1711, Nov. 2005.
- [26] R.C. Michelson and M.A. Naqvi, "Beyond Biologically Inspired Insect Flight", in von Karman Institute for Fluid Dynamics RTO/AVT Lecture Series on "Low Reynolds Number Aerodynamics on Aircraft Including Applications in Emerging UAV Technology", pp. 1-19, Brussels, Belgium, 2003.
- [27] R. M. Murray, Z. Li, and S. S. Sastry, "A Mathematical Introduction to Robotic Manipulation", CRC, Boca Raton, FL, 1994.
- [28] G. Nalbach, "The halteres of the blowfly *Calliphora*: I. Kinematics and dynamics", *Journal of Comparative Physiology A*, Vol. 173, pp. 293-300, 1993.
- [29] W. Reichardt and M. Egelhaaf, "Properties of individual movement detectors as derived from behavioural experiments on the visual system of the fly", in *Biological Cybernetics*, Vol. 58, No. 5, pp. 287-294, 1988.
- [30] S.P. Sane and M.H. Dickinson, "The control of flight force by a flapping wing: Lift and drag production", *The Journal of Experimental Biology*, Vol. 204, pp. 2607-2626, 2001.
- [31] S.P. Sane, "The aerodynamics of insect flight", *The Journal of Experimental Biology*, Vol. 206, pp. 4191-4208, 2003.
- [32] S. S. Sastry, "Nonlinear Systems: Analysis, Stability and Control", Springer, New York, 1999.
- [33] L. Schenato, W. C. Wu and S. S. Sastry, "Attitude Control for a Micromechanical Flying Insect via Sensor Output Feedback", *IEEE Trans. on Robotics and Automation*, Vol.20, No. 1, pp. 93-106, Feb. 2004.
- [34] H. Schuppe and R. Hengstenberg, "Optical properties of the ocelli of *Calliphora erythrocephala* and their role in the dorsal light response", *Journal of Comparative Biology A*, Vol. 173, pp. 143-149, 1993.
- [35] G.K. Taylor, "Mechanics and aerodynamics of insect flight control", *Biological Review*, Vol.76, No. 4, pp. 449-471, 2001.
- [36] Victoria Museum, URL: <http://www.museum.vic.gov.au/>.
- [37] E. Wajnberga and G. Cernicchiaro and D. Acosta-Avalosb and L. J. El-Jaicka and D. M. S. Esquivel, "Induced remanent magnetization of social insects", *Journal of Magnetism and Magnetic Materials*, Vol. 226-230, pp. 2040-2041, 2001.
- [38] J. Wessnitzer and B. Webb, "Multimodal sensory integration in insects: towards insect brain control architectures", *Bioinspiration & Biomimetics*, Vol. 1, pp. 63-75, 2006.
- [39] W. C. Wu, R. J. Wood and R. F. Fearing, "Halteres for the Micromechanical Flying Insect", in Proc. of IEEE Intl. Conf. on Robotics and Automation (ICRA), pp. 60-65, 2002.
- [40] W. C. Wu, L. Schenato, R. J. Wood and R. F. Fearing, "Biomimetic Sensor Suite for Flight Control of MFI: Design and Experimental Results", in Proc. of IEEE Intl. Conf. on Robotics and Automation (ICRA), pp. 1146-1151, 2003.